



Characterization of ultrafine particles and the occurrence of new particle formation events in an urban and coastal site of the Mediterranean area

Adelaide Dinoi¹, Daniel Gulli², Kay Weinhold³, Ivano Ammoscato², Claudia R. Calidonna², Alfred Wiedensohler³, and Daniele Contini¹

¹Institute of Atmospheric Sciences and Climate of the National Research Council of Italy, ISAC-CNR, S. P. Lecce-Monteroni km 1.2, 73100 Lecce, Italy

²Institute of Atmospheric Sciences and Climate of the National Research Council of Italy, ISAC-CNR, Zona Industriale, 88046 Lamezia Terme (CZ), Italy

³Leibniz Institute for Tropospheric Research, 04318, Leipzig, Germany

Correspondence: Adelaide Dinoi (a.dinoi@isac.cnr.it)

Received: 29 July 2022 – Discussion started: 18 August 2022

Revised: 4 January 2023 – Accepted: 19 January 2023 – Published: 13 February 2023

Abstract. In this work, new particle formation events (NPFs) occurring at two locations in southern Italy, the urban background site of Lecce (ECO station) and the coastal site of Lamezia Terme (LMT station), are identified and analyzed. The study aims to compare the properties of NPF events at the two sites, located 225 km away from each other and characterized by marked differences in terms of emission sources and local weather dynamics. Continuous measurements of particle number size distributions, in the size range from 10 to 800 nm, were performed at both sites by a mobility particle size spectrometer (MPSS). The occurrence of NPF events, observed throughout the study period that lasted 5 years, produced different results in terms of frequency of occurrence: 25 % of the days at ECO and 9 % at LMT. NPF events showed seasonal patterns: higher frequency during spring and summer at the urban background site and the autumn–winter period at the coastal site. Some of these events happened simultaneously at both sites, indicating the occurrence of the nucleation process on a large spatial scale. Cluster analysis of 72 h back trajectories showed that during the NPF events the two stations were influenced by similar air masses, most of which originated from the north-western direction. Local meteorological conditions characterized by high pressure, with a prevalence of clear skies, low levels of relative humidity ($RH < 52\%$), and moderate winds ($3\text{--}4\text{ m s}^{-1}$) dominated the NPF events at both sites. Notable differences were observed in SO_2 and $\text{PM}_{2.5}$ concentrations and H_2SO_4 proxy levels, resulting in $\sim 65\%$, $\sim 80\%$, and 50 % lower levels at LMT compared to ECO, respectively. It is likely that the lower level of that which is recognized as one of the main gas precursors involved in the nucleation process could be responsible for the smaller NPF frequency of occurrence ($\sim 60\%$ less than ECO) observed in LMT.

1 Introduction

The formation of new particles (NPF) by nucleation of gas-phase species and consecutive growth is an important atmospheric process that contributes to producing high levels of ultrafine particles (UFPs, diameter $< 100\text{ nm}$). Together with primary sources, natural and anthropogenic, the nucleation represents a significant source of secondary ultrafine aerosol

particles and cloud condensation nuclei (Merikanto et al., 2009; Yu et al., 2020), accounting for about 50 % of the production of particle number concentration on a global scale. Due to their size, high number concentration, and chemical composition, these particles have profound implications on the environment, climate, and public health (Zhang et al., 2015; Sartelet et al., 2022), which emphasizes their relevance.

The formation of new particles was observed and investigated in various geographic locations under different atmospheric and environmental conditions, from which common characteristics and different peculiarities emerged (Baalbaki et al., 2021; Jokinen et al., 2022; Yadav et al., 2021; Franco et al., 2022).

The new particle formation can occur on a local scale, typically characterized by an intense burst (strong intensity) of secondary particle formation of short duration and without subsequent growth (Dai et al., 2017), usually related to local anthropogenic emissions (Hussein et al., 2014), or else it can manifest as a part of an event which takes place on a large spatial scale (regional event). In this case, the nucleation process can originate from several hundred kilometers away from the measurement site (Dall'Osto et al., 2013; Németh and Salma, 2014; Zhu et al., 2014), and the newly formed particles can be contemporarily observed in multi-location measurements. It was noted that most NPF events occurred in analogous conditions, under the influence of air masses with the same origin and enriched with sulfur-rich precursors (Kalkavouras et al., 2020) and exhibiting similar dynamic characteristics. NPF events were usually detected in ground-based measurement stations, but a number of observations were also performed at high altitudes on mountain tops (Rose et al., 2015; Bianchi et al., 2016) by balloons and through aircraft (Schroder and Strom, 1997; Mirme et al., 2010), leading to the hypothesis that the nucleation process can be triggered within the atmospheric column at different heights (Boulon et al., 2011; Minguillón et al., 2015; Querol et al., 2017), both throughout the boundary layer and in the free troposphere. At upper atmospheric levels, nucleation would be facilitated by the higher dilution of the pollutants (low condensation sink) and by enhanced photochemical conditions. Once nucleated, the particles can be transported over long distances by the circulation of air masses. Where and at which altitude the mechanism is triggered is still unclear (Boulon et al., 2011), but in this process atmospheric dynamics could play a crucial role in the mixing of precursor gases and/or pre-existing particles, influencing their occurrence and spatial distribution (Wehner et al., 2015).

To date, the variability of the conditions and the complexity of the phenomenon make our knowledge of this process still fragmentary in many aspects. While it is well known that solar intensity, low relative humidity, and the availability of high levels of aerosol nucleation precursors (sulfur dioxide, ammonia, amines, volatile organic compounds (VOCs)) are common features in the NPFs (Wu et al., 2021), the chemical and physical mechanisms involved in the process remain uncertain, and further insights are required.

In this paper, we summarize the results of a long-term study on the new particle formation events carried out at two sites in southern Italy, Lecce (ECO station) and Lamezia Terme (LMT station). To the best of our knowledge, this work represents one of the few long-term studies on NPF events conducted in the Mediterranean area and the first one

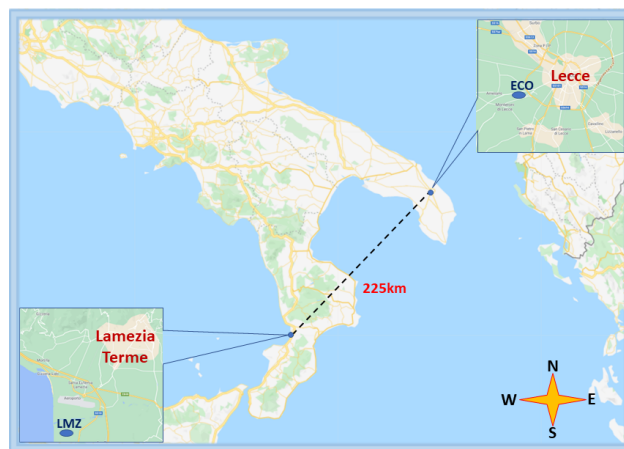


Figure 1. Map of the examined area with the locations of the two environmental–climate observatories, ECO and LMT. The map was retrieved from Google (map data © 2022).

conducted in Italy. Based on a 5-year period, simultaneous measurements of aerosol particle number size distribution were analyzed with the aim of characterizing, investigating, and comparing the relationship of NPF events with meteorological and pollution data at a coastal and an urban background site. To support interpretations, simultaneous measurements of SO_2 and $\text{PM}_{2.5}$ ambient concentrations were carried out at both ground-monitoring stations. The role of air mass and local meteorological factors were also investigated.

2 Measurements and methods

2.1 Measurement sites and instrumentation

Measurements of particle number size distribution (PNSD) were made from January 2015 to December 2019 at two sites in southern Italy, Lamezia Terme Observatory (LMT; 38.88°N , 16.23°E ; 6 m a.s.l.) in the Calabria region and Lecce Observatory (ECO; 40.20°N , 18.07°E ; 50 m a.s.l.) in the Puglia region. The locations of the measuring sites are depicted in Fig. 1. ECO and LMT, both regional stations of GAW/ACTRIS (Global Atmospheric Watch/Aerosols, Clouds, and Trace Gas Research Infrastructure) networks, are representative of urban backgrounds and suburban and coastal sites, respectively. ECO observatory is located inside the University Campus (Dinoi et al., 2020), about 5 km southwest of the municipality of Lecce, while the LMT observatory is located about 17 km from the urban city and about 600 m inland from the Tyrrhenian coastline, at an elevation of 6 m a.s.l. (above sea level). The two sites are about 225 km as the crow flies. The municipalities cover areas of 238 km^2 (Lecce) and 160 km^2 (Lamezia), with populations of 95 000 and 70 452 inhabitants, respectively. Their climate is Mediterranean, albeit characterized by different local me-

teological conditions. Being on the coast, the local weather of LMT is influenced by a system of “land–sea” breezes that guarantees a temperate climate and continuous ventilation throughout the year that favors an effective dilution of air pollutants. Different emission sources (more details from Cristofanelli et al., 2018; Calidonna et al., 2020; Dinoi et al., 2021b) affect the two sites. The main aerosol sources in the ECO observatory are the emissions of vehicular traffic and biomass combustions, which are added to natural and anthropogenic long-range contributions (Donateo et al., 2018; Conte et al., 2020). The site is characterized by frequent conditions of clear skies throughout the whole year, with mild autumn–winter seasons and warm spring–summer seasons. The LMT observatory is located far from the urban agglomeration and therefore is not directly affected by the emissions deriving from the main anthropogenic activities.

Aerosol PNSDs from 10 to 800 m, with a time resolution of 5 min, were collected using a TROPOS-type custom-built MPSS (mobility particle size spectrometer), designed and manufactured according to EUSAAR/ACTRIS recommendations (Wiedensohler et al., 2012). It is a closed-loop system, with a 5 : 1 ratio between the sheath and aerosol flow, where the sample air is drawn into the instrument at a flow rate of 1 L min^{-1} , while the sample humidity is regulated below 40 % by a Nafion dryer. The two MPSSs consist of a bipolar diffusion charger (Ni-63), a differential mobility analyzer (Vienna-type DMA, length 28 cm), and a condensation particle counter (CPC, model TSI 3772, TSI Inc., USA). The instrumentation used, the calibration procedures (carried out periodically), and data quality control were the same at the two stations. The quality of the measurements of both instruments was routinely checked, and all data were corrected for particle losses by diffusion and multiple charged particles according to the recommendations of Wiedensohler et al. (2012). Concentrations of sulfur dioxide (SO_2) were measured using Thermo Instruments analyzers, TEI 43i, and $\text{PM}_{2.5}$ mass concentrations using low-volume samplers with a β -ray attenuation method (SWAM 5a Dual Channel Monitor (FAI Instruments)). Local meteorological parameters, air temperature (T), relative humidity (RH), precipitation (rain), wind speed (WS), and wind direction (WD) were monitored by automatic weather stations (Vaisala WXT 520) located in the two observatories, while solar radiation (solar flux) was collected by CNR 4 net radiometers (Kipp & Zonen). Air mass back trajectories were calculated using the HYSPLIT 4 model developed by NOAA/ARL, a single-particle Lagrangian-trajectory dispersion model (Stohl, 1998).

2.2 Data analysis

Classification of NPF events was performed by visual inspection of daily contour plots (Dal Maso et al., 2005). Examining the time evolution of the particle number size distribution, three main classes were detected: NPF events, non-events, and undefined events. NPF events contain cases

where a significant increase in the number concentrations of ultrafine particles and growth toward larger diameters was observed for at least 3–4 h continuously, displaying the shape of a “banana”. “Non-events” are the days without new particle formation, while “undefined events” group ambiguous cases with unclear formation and growth or the occurrence of newly formed particles below 20 m without the next phase of growth.

Particle growth rate (GR) was calculated from time evolution of the mean geometric diameter D_p in the size range of 10–20 m, using Eq. (1) (Kulmala et al., 2012):

$$\text{GR}(\text{nm h}^{-1}) = (D_{p2} - D_{p1}) / (t_2 - t_1), \quad (1)$$

where D_{p1} and D_{p2} are the geometric diameter at the start time t_1 and end time t_2 of the growth event. Using the maximum concentration method (Lehtinen and Kulmala, 2003), we identified the time when the concentration was at the maximum in each size bin of the measured particle number size distributions. The growth rates were obtained as the slope of the linear fit of the times with the corresponding geometric mean diameters of the size bin particles.

The condensation sink, CS (s^{-1}), quantifies how rapidly a condensable gaseous compound condenses on available aerosol particles (Kerminen et al., 2018), depending on the effective surface area of pre-existing particles. CS was calculated using the methods available in the literature (Dal Maso et al., 2005, and references therein), considering sulfuric acid (H_2SO_4) as the condensable species:

$$\text{CS} = 2\pi D \sum_{D'_p} \beta_m(D'_{pi}) D'_{pi} N_i, \quad (2)$$

where D is the diffusion coefficient for H_2SO_4 , N_i is the particle number concentration with diameter D'_{pi} of the size bin i , and β_m is the transition correction factor (Fuchs and Sutugin, 1971).

The formation rate, J (J_{10} ; $\text{cm}^{-3} \text{ s}^{-1}$), defined as the flux of changes in particle number concentration within the nucleation mode size range (10–20 m), was estimated by (Dal Maso et al., 2005; Kulmala et al., 2012)

$$J = \frac{dN_{\text{nuc}}}{dt} + \text{CoagS}_{\text{nuc}} \times N_{\text{nuc}} + \frac{\text{GR}}{\Delta dp} N_{\text{nuc}}, \quad (3)$$

where (dN_{nuc}/dt) is the temporal change rate of nucleation mode particle number concentration, and $(\text{CoagS}_{\text{nuc}} \cdot N_{\text{nuc}})$ is the loss caused by collision process and by the growth process ($\text{GR} \cdot N_{\text{nuc}} / \Delta dp$).

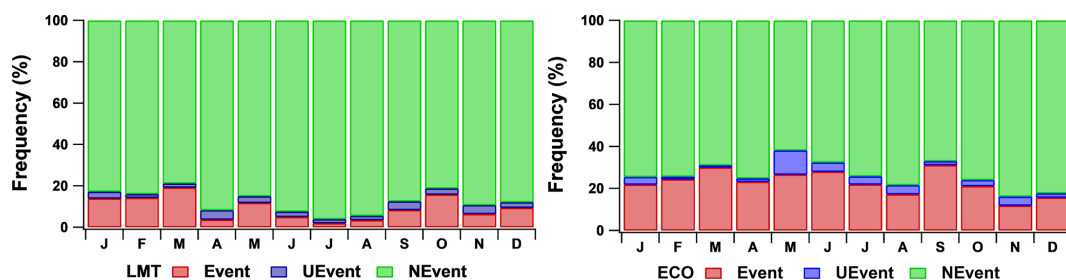
Sulfuric acid (H_2SO_4) is considered to be a key precursor for new particle formation; therefore, its concentrations were derived by calculating the H_2SO_4 proxy, without scaling factor, using the method presented by Petäjä et al. (2009):

$$[\text{H}_2\text{SO}_4] \propto \frac{\text{SO}_2 \times \text{SRad}}{\text{CS}}, \quad (4)$$

where SO_2 is the sulfur dioxide concentration, SRad is the solar radiation flux, and CS the condensation sink.

Table 1. Number of available days (N) and relative frequencies (f %) of each class, NPF event, non-event, and undefined event detected in ECO and LMT observatories.

Day classification	LMT (total = 1440)		ECO (total = 1423)	
	Number	Frequency (%)	Number	Frequency (%)
NPF events	124	9	352	25
Non-events	1272	88	1019	71
Undefined events	44	3	52	4

**Figure 2.** Monthly percentage of occurrence of events (red bars), undefined events (blue bars), and non-events (green bars) related to available measurement days at LMT and ECO.

3 Results and discussions

3.1 Classification of NPF events

The relative frequency of the different classes, events, non-events, and undefined events was calculated for both sites and summarized in Table 1. Over 5 years of measurements, we had a data coverage of $\sim 78\%$, where the available measurement days were 1423 at ECO and 1440 at LMT. The missing days were due to technical and/or maintenance problems of the MPSS or measurement failures and mainly concerned the months of February and March for LMT and January for ECO. Among the available data, 25 % and 9 % of days were identified as NPF events, while 4 % and 3 % were identified as undefined events at ECO and LMT, respectively. We found that the percentage frequency of NPF events is higher in ECO than in LMT, with differences in the monthly and seasonal occurrence of the events (Fig. 2). At the ECO site, the highest frequencies of NPF events were observed in March and September ($\sim 30\%$), and the lowest were observed in November and December (12 %–16 %), showing similar results to those found in a shorter measurement period presented by Dinoi et al. (2021a). At LMT, March (19 %) and October (16 %) showed the highest frequencies, while July and August showed the lowest ones (2 %–3 %). Consequently, this is reflected in a different seasonality of events, more frequent in spring and summer in ECO and in autumn and winter in LMT. Of all the events detected during the study period, 50 were observed simultaneously at both sites. Due to the complementary frequency, most of them occurred in the colder months – $\sim 23\%$ in winter and spring, 14 % in summer, and 39 % in autumn. The annual frequen-

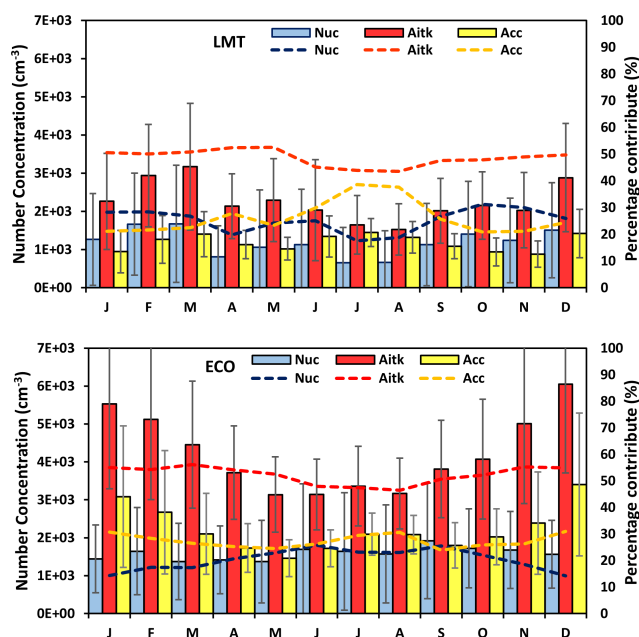
cies of NPFs (9 % and 25 %) are in good agreement with frequencies (10 %–36 %) found in other studies based on long-term measurements and carried out in the Mediterranean area (Kopanakis et al., 2013; Kalivitis et al., 2019; Hussein et al., 2020; Kalkavouras et al., 2020; Baalbaki et al., 2021). The seasonal variability observed in the ECO site was also similar to that found in several other locations (in Europe and around the world) and can be ascribed to the higher emissions of biogenic aerosol precursor compounds and photochemical processes promoted by the higher temperature during the warmer months (Asmi et al., 2016). However, the opposite trend displayed by the LMT site is not a novelty, since it has also been observed, albeit less frequently, in other southern Europe sites. In Spain and Greece, for example, Bousiotis et al. (2021) found the occurrence of a larger number of NPF events just during winter, and that might be linked to the specific meteorological conditions of the study area.

3.2 Atmospheric particle number concentration (PNC)

A statistical overview of the concentrations and contributions of three diameter modes particles – nucleation ($N_{\text{nuc}} = N_{10-20}$), Aitken ($N_{\text{Aitk}} = N_{20-100}$), and accumulation ($N_{\text{acc}} = N_{100-800}$) – to total particle number concentration ($N_{\text{tot}} = N_{10-800}$) was made. As summarized in Table 2 (arithmetic means ± 1 standard deviation, medians, and percentiles (25th–75th)), the mean value of total PNC was $(4.4 \pm 2.2) \times 10^3 \text{ cm}^{-3}$ at LMT and $(7.8 \pm 3.4) \times 10^3 \text{ cm}^{-3}$ at ECO. Although significantly higher concentrations (about 40 %) were found at the urban background site compared to the coastal site, the contribution of each particle fraction to total particle number concentration was very similar: 24 %,

Table 2. Arithmetic means \pm 1 standard deviation and median (25th–75th) percentiles of total, accumulation, Aitken, and nucleation PNC (cm^{-3}) for both sites.

	N_{nuc} (10^3 cm^{-3})	N_{Aitk} (10^3 cm^{-3})	N_{acc} (10^3 cm^{-3})	N_{tot} (10^3 cm^{-3})
LMT	1.1 ± 1.0 0.7 (0.3–1.5)	2.2 ± 1.1 1.9 (1.4–2.7)	1.2 ± 0.6 1.0 (0.7–1.0)	4.4 ± 2.2 4.0 (2.8–5.6)
ECO	1.6 ± 1.0 1.3 (0.9–1.9)	4.1 ± 1.8 3.7 (2.8–4.8)	2.1 ± 1.4 1.8 (1.2–2.6)	7.8 ± 3.4 7.1 (5.5–9.3)

**Figure 3.** Average monthly variation (bars) of the nucleation, Aitken, and accumulation mode particle number concentrations over the whole period of study at LMT and ECO. The dashed lines represent the monthly percentage contribution of each particle fraction to total particle number concentration.

49 %, and 27 % in LMT and 20 %, 52 %, and 28 % in ECO for nucleation, Aitken, and accumulation mode particles, respectively. In both cases, Aitken mode particles represented the largest fraction of particle number concentrations.

The levels measured at the two sites are within the range reported for similar locations observed in other European sites (Putaud et al., 2010; Asmi et al., 2011; Kalivitis et al., 2019; Casquero-Vera et al., 2020; Kalkavouras et al., 2020). The monthly variability of PNC, averaged over the whole study period, is shown in Fig. 3. In ECO and LMT, the highest monthly average concentrations of Aitken mode particles were observed during winter ($\sim 5.6 \times 10^3$ and $\sim 2.7 \times 10^3 \text{ cm}^{-3}$), approximately 45 % and 35 % higher than in summer ($\sim 3.2 \times 10^3$ and $\sim 1.7 \times 10^3 \text{ cm}^{-3}$) in ECO and LMT, respectively. In ECO, accumulation mode particles ranged from $\sim 1.7 \times 10^3 \text{ cm}^{-3}$ in spring to $\sim 3.1 \times 10^3 \text{ cm}^{-3}$ in winter, while in LMT they ranged from $\sim 9.8 \times 10^2 \text{ cm}^{-3}$

in autumn to $\sim 1.4 \times 10^3 \text{ cm}^{-3}$ in summer. The increase in N_{acc} concentration during the summer can be ascribed to the dry conditions that characterize the Mediterranean summers (Pikridas et al., 2018). Nucleation mode particles displayed a similar seasonal pattern to Aitken mode particles in LMT (from $\sim 8.0 \times 10^2 \text{ cm}^{-3}$ in summer to $\sim 1.4 \times 10^3 \text{ cm}^{-3}$ in winter), while in ECO values slightly higher were observed during spring–summer ($\sim 1.9 \times 10^3 \text{ cm}^{-3}$) than in winter ($\sim 1.3 \times 10^3 \text{ cm}^{-3}$). The higher concentrations recorded during cold months are generally associated with enhanced anthropogenic emissions from fossil fuel combustion and biomass burning due to residential heating and unfavorable meteorological conditions for pollution dispersion.

A clear diurnal pattern for each mode particle number concentration was observed in every season. Figure 4 shows the trend of each mode fraction, considering separately the days of NPF events (E, solid line) and the days of non-events (NE, dashed line). The timing of measurements is expressed in solar time (UTC + 1). Nucleation, Aitken, and accumulation mode particles have very similar behavior during non-events, and except for the different concentrations, both sites show a pronounced diurnal cycle with a morning and evening peak. The two peaks are shifted by 1 h between spring–summer and autumn–winter because of daylight savings time and are mainly linked to vehicular emissions, most intense during the morning and evening rush hour. In addition, the evening peaks of Aitken and accumulation mode particles in winter and autumn can be linked to domestic heating emissions, mainly biomass burning, which is considered an important source of ultrafine particles in urban sites. In cold months, these particles tend to accumulate during the night due to the reduced boundary layer compared to the daytime layer. These peaks are also present in LMT but are less intense due to the greater distance of the site from the urban center. Regarding event days, in both sites, together with the two peaks of rush hour, nucleation mode particles present further peaks around noon, which are more marked in summer, spring, and winter in ECO and in spring, summer, and autumn in LMT. Less pronounced are those in winter and autumn in LMT and ECO, respectively.

Similar observations have been reported in Cusack et al. (2013), Kalivitis et al. (2019), Kalkavouras et al. (2020), and Dinoi et al. (2020, 2021a) for the western Mediterranean sites where the diurnal variation in nucleation mode parti-

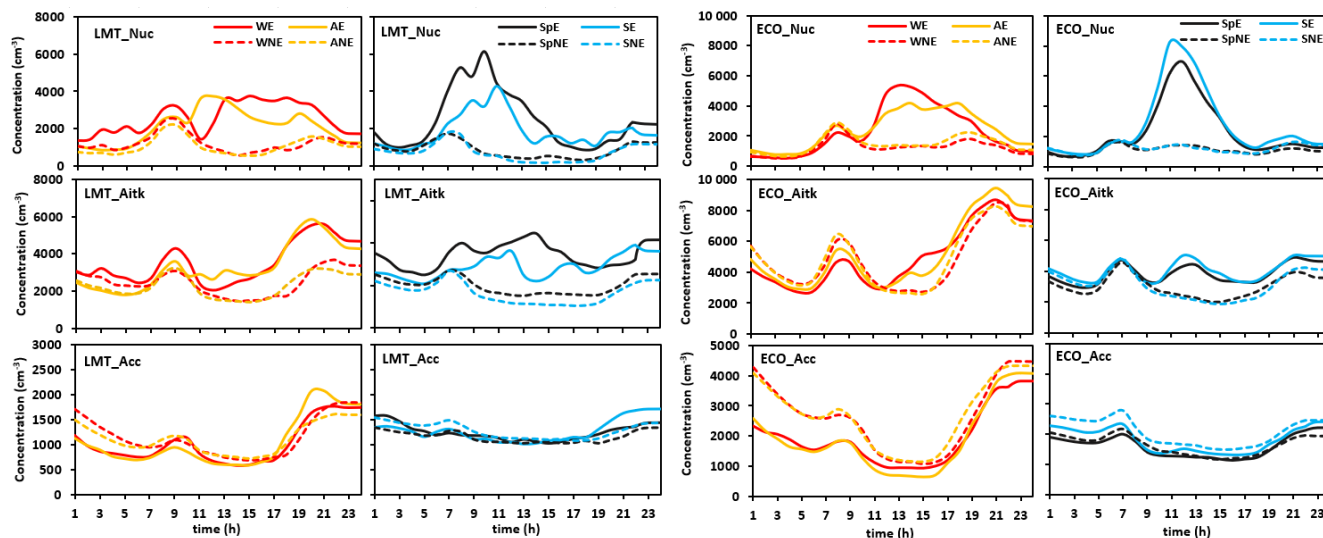


Figure 4. Average diurnal variation in nucleation, Aitken, and accumulation mode particle number concentrations (from top to bottom) over the whole period of study at LMT and ECO. Solid lines are for NPF events days (E), and dashed lines are for non-events days of (NE); red is for winter, gray is for spring, blue is for summer, and yellow is for autumn.

cles presents a clear maximum at noon under both polluted and clean conditions. The contribution of the NPF process to the number concentration is also observed in the Aitken mode particles, more noticeable in the LMT site with 30 % in autumn–winter and 41 % in spring–summer and with 21 % in only spring–summer in the ECO site. In Table 3 are the reported mean values ± 1 standard deviation of nucleation, Aitken, and accumulation of PNC (cm^{-3}) related to event days (E) and non-event days (NE) for each season (winter, W; spring, Sp; summer, S; and autumn, A) in both sites. Nucleation mode particles show increases of 52 %, 65 %, 61 %, and 49 % in winter, spring, summer, and autumn in LMT and of 47 %, 52 %, 55 %, and 39 % in ECO. These results highlight that the formation of new particles contributes to the overall particle population more in the warm months and more significantly in the coastal site than in the urban background site, probably because the urban site is also affected by local emissions of ultrafine particles that tend to suppress the NPF process.

No contribution is observed in the concentration of accumulation mode particles where, especially in the first half of the day, the concentrations were higher on non-event than event days, especially at the ECO site. This could explain the different frequency of events that characterized the two sites in these seasons, assuming that the NPF events were favored on those days with lower particle number concentrations (Salma et al., 2017).

The relative increase in particle number concentration due to the NPF process was also quantified with the nucleation strength factor (NSF) proposed by Salma et al. (2016, 2017) and Salma and Németh (2019). It measures the effects of nucleation events on ultrafine particles at a site considering two

factors: NSF_{NUC} , which provides a measure of the concentration increment on nucleation days exclusively caused by NPFs, and NSF_{GEN} , which gives a measure of the overall contribution of NPFs over a longer time span. In this work, we considered only NSF_{NUC} , calculated following Eq. (5):

$$\text{NSF}_{\text{NUC}} = \frac{(N_{10-100})/(N_{100-800})_{\text{E}}}{(N_{10-100})/(N_{100-800})_{\text{NE}}}, \quad (5)$$

where N_{10-100} and $N_{100-800}$ are the concentration ratios for nucleation days at the numerator, and the N_{10-100} and $N_{100-800}$ are the concentration ratios for non-nucleation days at the denominator. Depending on the value, $\text{NSF}_{\text{NUC}} < 1.0$, $1.0 < \text{NSF}_{\text{NUC}} < 2.0$, or $\text{NSF}_{\text{NUC}} > 2.0$, the nucleation process can be considered negligible, comparable to the other sources or the main contributor. In LMT the mean values of NSF_{NUC} were 2.0, 2.1, 2.3, and 1.9, while in ECO they were 1.7, 1.6, 1.9, and 1.9 in winter, spring, summer, and autumn, respectively. From the coastal to urban background site, we found a decrease in the contribution of NPF events to particle number, like what was observed by Salma et al. (2017) between the near-city background (2.3) and the city center (1.6) of Budapest over 5 years. In the study of Bousiotis et al. (2021), at 13 sites from five countries in Europe, it was found that for almost all rural background sites, NSF_{NUC} was greater than 2 and reached 4 in a very clean site of Finland. Nemet et al. (2018) found lower values of NSF_{NUC} (1.58, 1.54, and 2.01) in the cities of Budapest, Vienna, and Prague, respectively, while in the Granada urban site, NSF_{NUC} was 1.05 (Casquero-Vera et al., 2021). The decrease in the contribution of NPF events to particle number, moving from a less-polluted to a more-polluted site, may be related to the higher contribution to particle number concentrations of

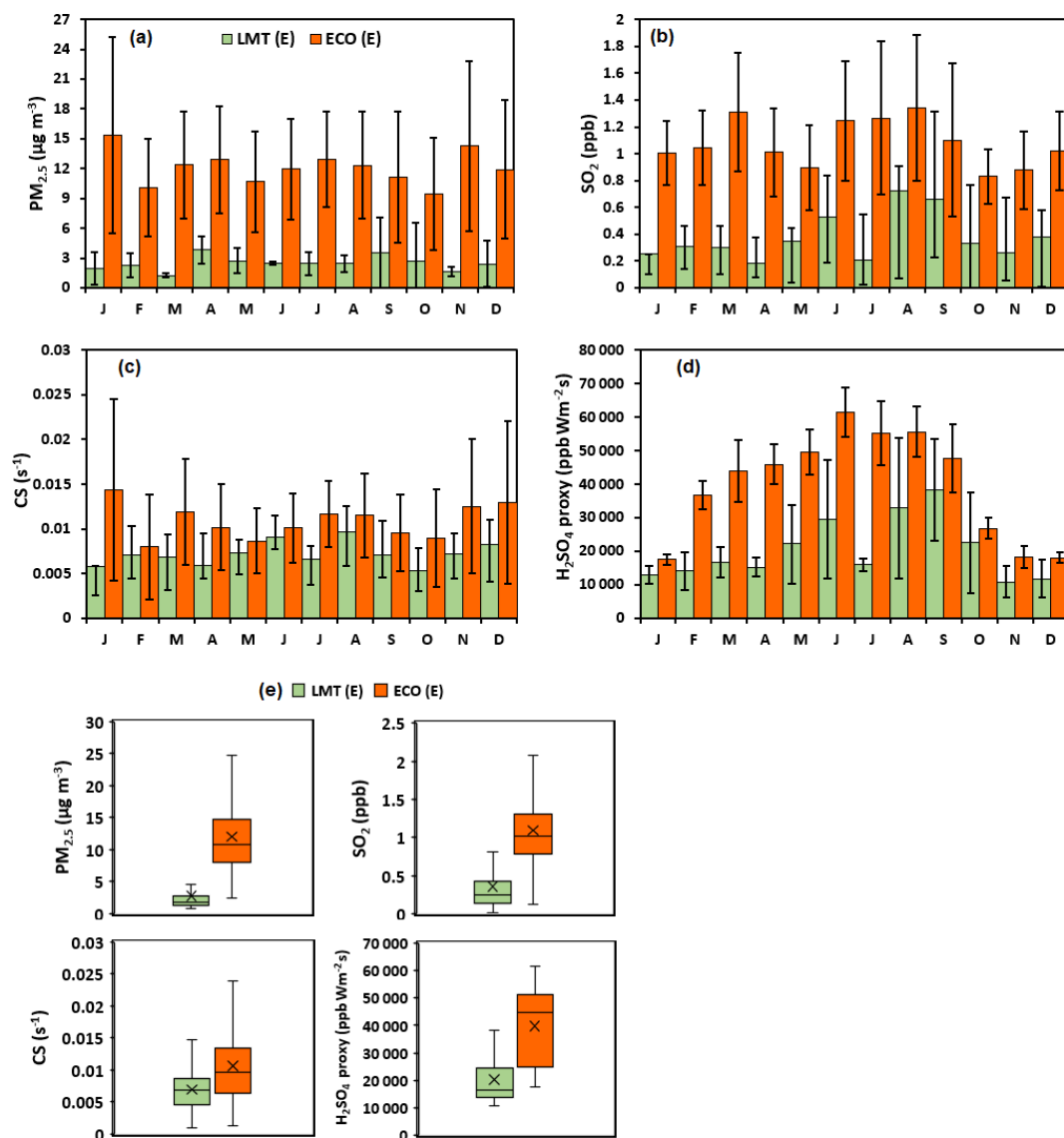


Figure 5. Monthly means of (a) $M_{2.5}$, (b) SO_2 , (c) CS, and (d) H_2SO_4 proxy related to event days for LMT (green) and ECO (red). The bars indicate the standard deviation. (e) Box plot of $PM_{2.5}$, SO_2 , CS, and H_2SO_4 proxy associated with event days for LMT (green) and ECO (red). The box shows the quartiles, the median (the line inside the box), the mean (the star), and the 90th and 10th percentiles (the whiskers).

Table 3. Arithmetic means ± 1 standard deviation of nucleation, Aitken, and accumulation PNC (cm^{-3}) related to event days (E) and non-event days (NE) for each season (winter, W; spring, Sp; summer, S; and autumn, A) and for both sites.

	LMT			ECO		
	N_{nuc} ($10^3 cm^{-3}$)	N_{Aitk} ($10^3 cm^{-3}$)	N_{acc} ($10^3 cm^{-3}$)	N_{nuc} ($10^3 cm^{-3}$)	N_{Aitk} ($10^3 cm^{-3}$)	N_{acc} ($10^3 cm^{-3}$)
W (E)	2.5 ± 0.8	3.5 ± 1.1	1.0 ± 0.4	2.3 ± 1.6	4.9 ± 1.9	1.9 ± 0.9
W (NE)	1.2 ± 0.5	2.4 ± 0.7	1.1 ± 0.4	1.2 ± 0.6	4.8 ± 1.8	2.6 ± 1.2
Sp (E)	2.4 ± 1.5	3.4 ± 0.6	1.2 ± 0.2	2.2 ± 1.8	3.8 ± 0.6	1.6 ± 0.3
Sp (NE)	0.8 ± 0.4	2.0 ± 0.4	1.2 ± 0.2	1.1 ± 0.3	3.0 ± 0.7	1.6 ± 0.3
S (E)	1.8 ± 0.9	2.9 ± 0.5	1.3 ± 0.2	2.7 ± 2.2	4.1 ± 0.7	1.8 ± 0.4
S (NE)	0.7 ± 0.4	1.6 ± 0.5	1.3 ± 0.2	1.2 ± 0.3	3.1 ± 0.9	2.1 ± 0.4
A (E)	2.0 ± 0.9	3.3 ± 1.2	1.0 ± 0.5	2.4 ± 1.2	5.2 ± 2.2	1.9 ± 1.1
A (NE)	1.1 ± 0.4	2.3 ± 0.6	1.1 ± 0.3	1.5 ± 0.6	4.9 ± 1.9	2.7 ± 1.1

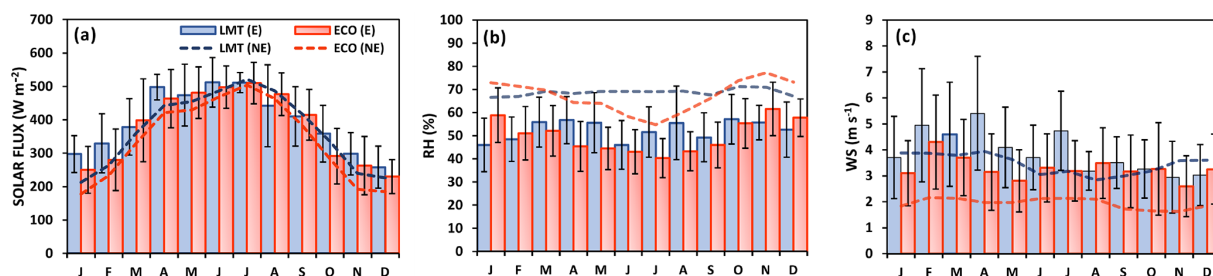


Figure 6. Monthly means of (a) solar flux, (b) relative humidity, and (c) wind speed related to event days (columns) and non-event days (dashed lines) for LMT (blue) and ECO (red). The bars indicate the standard deviation.

other sources, i.e., traffic and heating, and the associated increased condensation sink. These results point out that the particles produced by the NFS_{NUC} process can become the dominant sources in a clean environment compared to more-polluted areas.

3.3 Factors associated with NPF events

The growth rate (GR) and the particle formation rate (J) were analyzed to investigate the dynamic properties of NPF events. At the ECO site, the growth rate values ranged from 3 to 14 nm h⁻¹ (average 7.5 ± 3.3 h⁻¹), and J ranged from 0.6 to 8.6 cm⁻³ s⁻¹ (average 3.3 ± 3.1 cm⁻³ s⁻¹), while at LMT, the GR varied from 2.5 to 10 nm h⁻¹ (average 6.1 ± 2.3 m h⁻¹), and the J ranged from 0.3 to 6.2 cm⁻³ s⁻¹ (average 2.4 ± 1.8 cm⁻³ s⁻¹). The values of both parameters are comparable with what was reported for NPF events in other urban and coastal sites (Hussein et al., 2020; Kalivitis et al., 2019; Salma and Németh, 2019; Kalkavouras et al., 2020; Nieminen et al., 2018). In particular, similarities were found with some Mediterranean sites, such as the coastal station of Finokalia (GR ~ 5 nm h⁻¹, $J \sim 0.9$ cm⁻³ s⁻¹; Pikridas et al., 2012), the coastal, rural, suburban station of Akrotiri (GR ~ 6 nm h⁻¹, $J \sim 13$ cm⁻³ s⁻¹; Kopanakis et al., 2013), and the island of Cyprus (GR ~ 2.8 –5 nm h⁻¹, $J \sim 5$ –11.4 cm⁻³ s⁻¹; Debevec et al., 2018). The mean values of GR and J turned out to be higher at the ECO site than at the LMT site, and they showed a clear seasonal pattern with higher values during warm months, which not observed at LMT where both parameters did not show distinctive features. As reported by Nieminen et al. (2018), the production rate of nucleation particles is generally higher in urban sites than in remote, clean ones because of the greater availability of precursors deriving from greater anthropogenic activity. In particular, the higher values of GR and J in warm months can be attributed to the intensification of the photochemical activity and abundance of SO₂, which acts as a precursor of sulfuric acid. From this perspective, we investigated the effects of PM_{2.5}, CS, and SO₂ concentrations on the occurrence of NPF at both sites, where visible differences in pollution load (Fig. 5) were found. The average PM_{2.5} and SO₂ concentrations dur-

ing event days were 2.5 ± 1.5 μg m⁻³ (ranging from 2.0 to 3.8 μg m⁻³) and 0.4 ± 0.3 ppb (from 0.2 to 0.6 ppb) for LMT, while they were 12.0 ± 6.0 μg m⁻³ (from 9.5 to 15.3 μg m⁻³) and 1.1 ± 0.4 ppb (from 0.8 to 1.3 ppb) for ECO. These values were compared with mean values of PM_{2.5} and SO₂ measured on non-event days: 6.1 ± 2.5 μg m⁻³ and 0.2 ± 0.2 ppb in LMT, and 15.5 ± 8.0 μg m⁻³ and 0.9 ± 0.4 ppb in ECO. At both sites, statistically significant differences (p -value < 0.05 level, by Wilcoxon–Mann–Whitney test) emerged, highlighting the different roles they may have played in the new particle formation. CS, estimated from measurements of the particle number size distribution between 10 and 800 m, was $(0.7 \pm 0.3) \times 10^{-2}$ s⁻¹ (0.005–0.009 s⁻¹) for LMT and $(1.0 \pm 0.6) \times 10^{-2}$ s⁻¹ (0.008–0.01 s⁻¹) for ECO, within the range of coastal and urban environments (Salma et al., 2016; Kalivitis et al., 2019; Baalbaki et al., 2021). In this case, the comparison with values measured during non-event days – $(0.7 \pm 0.4) \times 10^{-2}$ s⁻¹ in LMT and $(1.3 \pm 0.5) \times 10^{-2}$ s⁻¹ in ECO – showed no noteworthy differences. The two sites displayed evident differences in both concentrations, with SO₂ ~ 65 %, PM_{2.5} ~ 80 %, and CS ~ 30 % being lower in LMT than ECO. This underlines how the two areas are affected in different ways by anthropogenic contributions and that the lower levels of SO₂ could be responsible for the reduced NPF frequency (~ 65 % less than ECO) observed in LMT. In general, particulate matter concentration has a direct effect on the condensation sink that quantifies how rapidly a condensable gaseous compound condenses on available aerosol particles (Kerminen et al., 2018). As is known, new particle formation is not favored by the high concentration of pre-existing particles because they increase condensation sink (CS) for vapors. Therefore, lower CS would favor nucleation proportionally to the amount of condensable vapors available (Saha et al., 2018). Sulfuric acid is identified as one of the key components directly connected to the NPF process (Sipilä et al., 2010). Because no direct measurements of it were done in this study, we investigate its role, considering the proxy of sulfuric acid (Eq. 4), without scaling factor (Petäjä et al., 2009). The proxy only allows us to estimate the order of the average concentration levels of H₂SO₄, and although the results obtained are subject

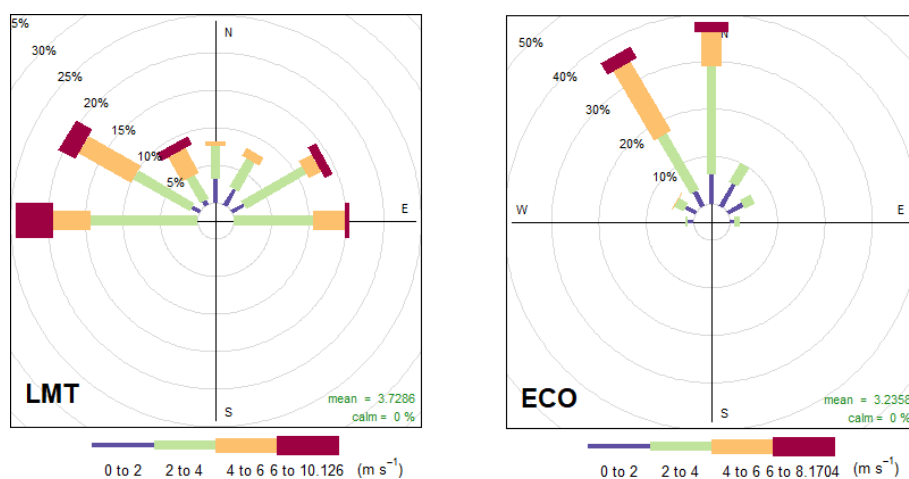


Figure 7. Wind roses related to event days for LMT and ECO observatories.

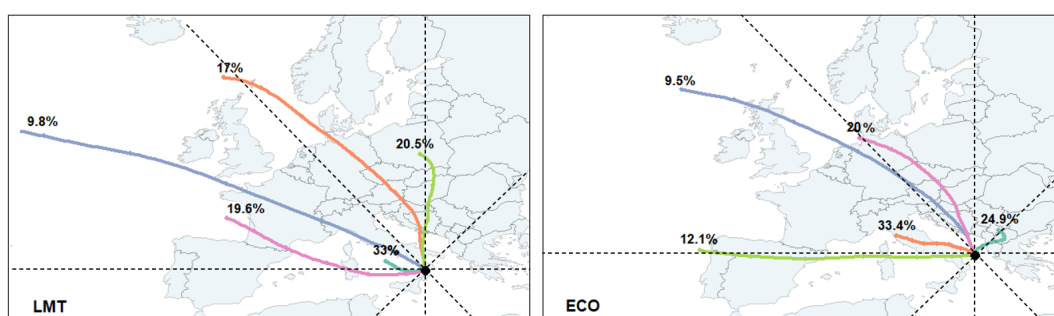


Figure 8. Cluster centroids retrieved from the 3 d analytical back trajectories reaching ECO and LMT at 500 m a.s.l. The maps were plotted using HYSPLIT integrated with the openair package.

to uncertainties, they can still provide indications of trends (Salma and Németh, 2019). The average monthly values of the H_2SO_4 proxy showed substantial differences between the two sites on event days (Fig. 5d): $40 \times 10^3 \text{ ppb Wm}^{-2} \text{ s}$ (ranging from 18×10^3 to $61 \times 10^3 \text{ ppb Wm}^{-2} \text{ s}$) at ECO and $20 \times 10^3 \text{ ppb Wm}^{-2} \text{ s}$ (from 11×10^3 to $38 \times 10^3 \text{ ppb Wm}^{-2} \text{ s}$) at LMT. These values are about 35 % higher than non-event days in both cases. The proxy values of H_2SO_4 are larger in warm months and are substantially higher, by a factor of 2, in the urban background than in the coastal site, mainly due to the values of CS and SO_2 . These last results are in accordance with GR and J values obtained for the two sites, where the low J and GR values at LMT could be associated with the low concentrations of H_2SO_4 (or other precursors). The conditions for the occurrence of NPF events are mainly driven by the ratio of the source and sink terms for the condensing vapors; therefore, a greater availability of this gas precursor could have favored the occurrence of NPF events at ECO, although the higher values of CS, as well as the lower levels, could have limited its development at LMT.

3.4 Meteorological conditions and air masses associated with NPF events

The comparison of the main meteorological parameters was carried out to better characterize the NPFs that occurred in terms of the local climate of the two study areas. The monthly average values of solar flux, relative humidity, and wind speed were calculated, starting with the daily averages. All NPF events happened in comparable weather conditions featuring high pressure, with a prevalence of clear skies, typical of the Mediterranean climate. Monthly mean values showed an intense solar flux in both LMT (from 260 to 512 Wm^{-2}) and ECO (from 230 to 510 Wm^{-2}) during events (columns). These values were very similar to those measured during non-event periods, except at the LMT site where higher mean values are observed in the colder months, though these differences are not statistically significant. During event days, the RH was comparable at the two sites: $52 \pm 4 \%$ in LMT and $50 \pm 7 \%$ in ECO. It was about 25 % lower than that on non-event days (Fig. 6b). This result is not a novelty because lower RH is usually observed during NPF events in both clean and polluted environments (Kerminen et al., 2018). On average, monthly wind speeds were higher during events at

both sites: $4 \pm 1 \text{ m s}^{-1}$ for LMT (from 2.9 to 5.4 m s^{-1}) and $3 \pm 1 \text{ m s}^{-1}$ for ECO (from 2.6 to 4.3 m s^{-1}), respectively, about 10 % and 40 % higher than the wind speed observed on non-event days (Fig. 6c). The difference is statistically significant only for ECO (p value < 0.05). Regarding the wind directions (Fig. 7) in ECO, the dominating wind direction was mainly from N–NNW, with a frequency of occurrence of 75 %, while in LMT, it was from E–NE and W–NW, with a frequency of occurrence of 30 % and 55 %, respectively, corresponding to a land–sea breeze system. Figure 7 was made using the openair package for R (Carslaw and Ropkins, 2012). The two prevalent wind directions, together with the higher wind speed (both on events and on non-event days), are typical of a coastal area where, generally, thanks to the circulation of the sea–land breeze, wind speed is approximately 20 % greater than in the innermost (inland) sites and is almost constant during the whole year (Jensen et al., 2017). The breezes influence the diffusion of atmospheric pollutants and their dilution, thus explaining the low and almost constant (lack of seasonality) levels of PM measured at LMT.

Also, the origin and pathways of air masses can contribute significantly to the occurrence of NPF processes (Wonaschütz et al., 2015). Depending on their advection pattern, air masses can be affected by emission sources, and chemical or physical processes able to influence the properties of the pollutants during transportation. With this aim, the role of air masses was investigated through the analysis of the back trajectories of all days identified as NPF events. The 72 h back trajectories were computed each day at 08:00 UTC with a 6 h resolution at the 500 m height arrival above ground level (a.g.l.), using the HYSPLIT 4, single-particle Lagrangian-trajectory dispersion model developed by NOAA/ARL (Draxler and Hess, 1998). We considered only the back trajectories at an altitude of 500 m because they can be better correlated with ground-based measurements and, therefore, more representative of the atmospheric boundary layer in which air pollutants are well mixed by horizontal and vertical advection. The analysis of the back trajectories allows us to gain qualitative information on the paths of the air masses associated with NPF events, and although they can be affected by an error estimated between 15 % and 30 % (Stohl, 1998; Draxler and Hess, 2004), for the purposes of this paper, we considered such inaccuracy to be negligible. The main transport pathways to the study sites were identified by cluster analysis of back trajectories. Figure 8, made using the openair package for R (Carslaw and Ropkins, 2012), shows six centroids, each representative of a group of trajectories, labeled according to the direction of the cluster, frequency of occurrence, and length. Short trajectories are indicative of slow-moving air masses while long trajectories are for fast flows; different lengths can have implications on a load of pollutants transported (associated) by air mass. As represented in Fig. 8, during the occurrence of NPF events the two stations were influenced by similar air

masses, most of which were enclosed in the north-western quadrant. Air masses arriving at LMT and originating from the north-northwestern sector exhibited an occurrence rate of 38 % (17 % long and 20.5 % medium trajectories), followed by 62 % of air masses from the west-northwest sector (9.8 % long, 19.6 % medium and 33 % short trajectories). At ECO, air masses originating from the north-northwestern sector showed a percentage of 20 % (medium trajectories), those from the west-northwest sector an occurrence of 55 % (21.6 % long and 33.4 % short trajectories), while another important contribution, 25 % (short trajectory), was associated to Eastern sector. All the air masses flew over both the European continental areas highly anthropized and the marine environment before reaching the receptor points. It is interesting to note the lack of air masses associated with NPF events coming from the southern sector. These air masses, because of their pathway, are usually characterized by high levels of dust and humidity able to counter the NPF process because they can suppress photochemical activity by scavenging reactive gases and condensable vapors (De Reus et al., 2000; Ndour et al., 2009).

We also focused on “common” NPF events considering only the air masses pathway related to these days detected during the study period. From 3-day back-trajectory analysis, it emerged that the back trajectories of common events exhibit similar characteristics in terms of origin and pathways to what already observed, but in addition, two different cases were detected, in the first the trajectory passes from ECO before reaching LMT, while in the other case, vice versa the air mass passes from LMT and then reaches ECO. Out of 50 common NPF events, 31 were in the first case and 19 in the second. Two representative examples of back trajectories for each case are depicted in Fig. 9 and show that there is not a preferential path that can characterize them because in both cases we find trajectories that come from both eastern and western Europe. These events occurred almost synchronously at the two sites, with a difference in starting time no greater than 30 min.

The factors that characterized the concomitant events of NPFs (Table 4) are similar to those observed for the non-concomitant events, with values of $\text{PM}_{2.5}$, SO_2 , CS, and H_2SO_4 proxy being lower in LMT than in ECO and with similar meteorological conditions. The simultaneous observation of these events indicates that the formation of new particles has a wide horizontal extension and can be seen as a large-scale phenomenon. It is probable that the air masses already contain particles that have been formed by nucleation somewhere and then transported, or during their travel, the air masses are enriched with gaseous precursors deriving from anthropogenic emissions and/or from biogenic production such as to foster (potentially) NPF processes, even in locations far from the sources.

These results emphasize the role that air masses have, not only in terms of transport of precursors but also in synoptic atmospheric conditions associated with them. In gen-

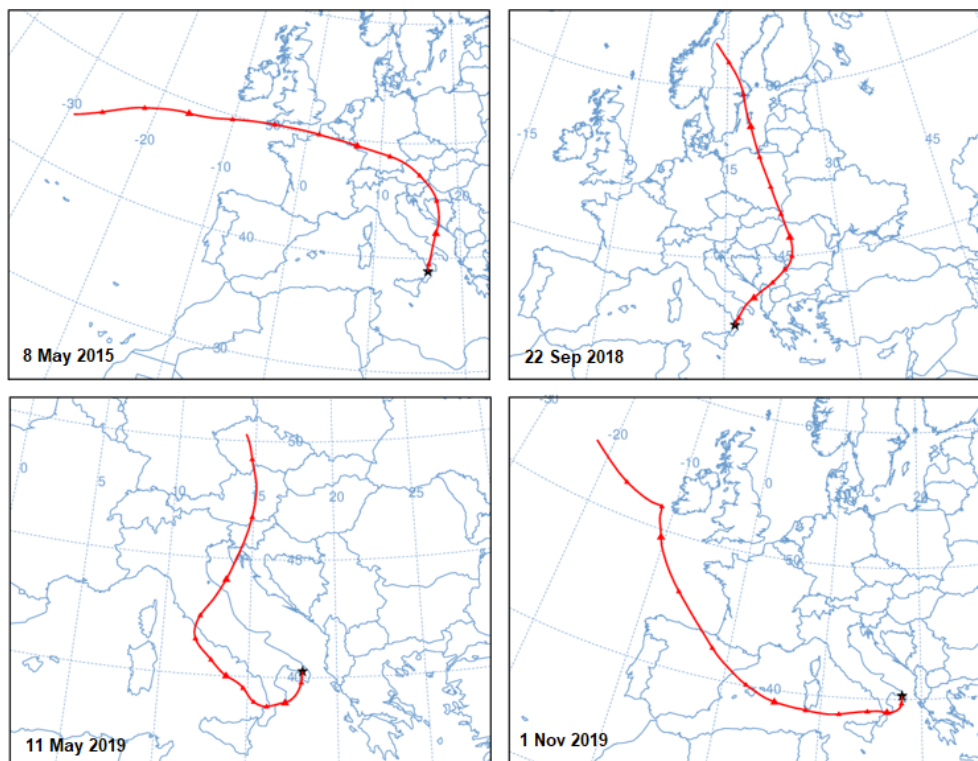


Figure 9. The 72 h back trajectories arriving at LMT (up) and ECO (down) during four simultaneous new particle formation events. The maps were retrieved from NOAA HYSPLIT Model.

Table 4. Arithmetic means ± 1 standard deviation and median (25th–75th) percentiles of different parameters: $\text{PM}_{2.5}$, SO_2 , CS, H_2SO_4 , GR, RH, WS, and SF for both sites.

	$\text{PM}_{2.5}$ ($\mu\text{g m}^{-3}$)	SO_2 (ppb)	$\text{CS} \times 10^2$ (s^{-1})	$\text{H}_2\text{SO}_4 \times 10^3$ ($\text{ppb W m}^{-2} \text{s}^{-1}$)	GR (nm h^{-1})	RH (%)	WS (m s^{-1})	SF (W m^{-2})
LMT	3.1 ± 2.6 2.0 (1.3–4.2)	0.3 ± 0.3 0.2 (0.2–0.4)	0.6 ± 3.0 0.6 (0.4–0.8)	21 ± 19 15 (10–23)	6.7 ± 2.6 6.2 (5.0–8.2)	48 ± 107 50 (40–56)	4.2 ± 1.4 3.9 (3.0–5.0)	394 ± 110 360 (313–496)
ECO	8.9 ± 4.8 8.0 (5.1–11.0)	0.9 ± 0.3 0.9 (0.8–1.0)	0.9 ± 0.6 0.8 (0.8–1.0)	38 ± 23 39 (26–62)	6.6 ± 2.0 6.6 (5.0–7.6)	49 ± 12 48 (41–56)	3.8 ± 1.7 3.5 (2.2–4.9)	365 ± 133 350 (340–470)

eral, these results underline the importance of specific atmospheric conditions (temperature, solar radiation, RH, origin of air mass, pollutant concentrations) under which the NPF events have occurred and emphasize how the observed differences are associated with the levels of pollution found in them. The more frequent NPF events at the urban background compared to the coastal site can be ascribed to a greater abundance of condensable species deriving from anthropogenic emissions which favor the growth of particles, increasing their chance of survival. Regarding the different seasonality of the events, while the trend at the urban site of ECO can be associated with the increased photochemical activity and the higher concentrations of different precursors during the warm months, the seasonality at the coastal site of LMT is more difficult to explain. Along with the lower

availability of precursors, local conditions could play an additional role as well. These may include synoptic systems such as increased turbulence during warm months and the different atmospheric composition (related to the proximity to the sea and the effects of land–sea breezes) due to which the newly formed particles could be more effectively suppressed, preventing further growth.

4 Conclusions

New particle formation events were studied and compared at two sites in southern Italy, ECO (Lecce) and LMT (Lamezia Terme) observatories, over a period of 5 years. The nucleation events occurred with a different frequency (25 % and

9%) and seasonality, being highest in spring–summer and autumn–winter at ECO and LMT, respectively.

Throughout the investigation period, 50 simultaneous NPF events (14% of the cases in ECO and 40% in LMT) were identified at both sites, many of which occurred in the colder months, indicating that the NPF process was affecting a large spatial extent. The NPF days were characterized by lower PM_{2.5} concentrations (~60% and 22%) and higher SO₂ concentrations (~50% and 20%) compared to non-event days in LMT and ECO, respectively, while the condensation sinks seemed not to be significantly different during events and non-event days. Marked differences in PM_{2.5}, SO₂, H₂SO₄ proxy, and CS levels were observed between the two sites, indicating the minor anthropogenic influence to which LMT is subjected. Common meteorological features were observed during NPF events that occurred in conditions of high pressure, low RH (~52%), and moderate wind speed (3–4 m s⁻¹). The study of the back trajectories associated with the events also highlighted a common origin of the air masses, both of continental and marine origin, from the north–northwest directions, suggesting that the chemical compounds involved in the NPFs could have been transported by the air masses. Our findings let us assume that the lower levels of SO₂ and H₂SO₄ proxy (–60% and –50% with respect to ECO) together with a different chemical composition of the aerosols and different local meteorology might be the reason for the lower frequency of events occurring in LMT (–60% with respect to ECO). The results presented in this paper are a contribution toward a better understanding of the complex NPF phenomena in the central Mediterranean area, which will require further investigation and measurement of the different precursors (such as ammonia, amines, VOCs) involved in the process that were not considered in this work.

Data availability. Data are available upon request.

Author contributions. AD and DC conceptualized the study design. AD, DG, and KW collaborated on data collection and post-processing. AD and DC prepared the draft. AD, DG, KW, IA, CC, AW, and DC collaborated on interpretation of results and wrote, read, commented on, and approved the final draft.

Competing interests. The contact author has declared that none of the authors has any competing interests.

Disclaimer. Publisher's note: Copernicus Publications remains neutral with regard to jurisdictional claims in published maps and institutional affiliations.

Acknowledgements. This work was supported by the project CIR01_00015 – PER-ACTRIS-IT “Potenziamento della componente italiana della Infrastruttura di Ricerca Aerosol, Clouds and Trace Gases Research Infrastructure – Rafforzamento del capitale umano” – Avviso MUR D.D. no. 2595 del 24.12.2019 Piano Stralcio “Ricerca e Innovazione 2015–2017”.

Financial support. This research has been supported by the Ministry of University and Research (MUR), grant no. CIR01_00015.

Review statement. This paper was edited by Veli-Matti Kerminen and reviewed by two anonymous referees.

References

- Asmi, E., Kivekäs, N., Kerminen, V.-M., Komppula, M., Hyvärinen, A.-P., Hatakka, J., Viisanen, Y., and Lihavainen, H.: Secondary new particle formation in Northern Finland Pallas site between the years 2000 and 2010, *Atmos. Chem. Phys.*, 11, 12959–12972, <https://doi.org/10.5194/acp-11-12959-2011>, 2011.
- Asmi, E., Kondratyev, V., Brus, D., Laurila, T., Lihavainen, H., Backman, J., Vakkari, V., Aurela, M., Hatakka, J., Viisanen, Y., Uttal, T., Ivakhov, V., and Makshtas, A.: Aerosol size distribution seasonal characteristics measured in Tiksi, Russian Arctic, *Atmos. Chem. Phys.*, 16, 1271–1287, <https://doi.org/10.5194/acp-16-1271-2016>, 2016.
- Baalbaki, R., Pikridas, M., Jokinen, T., Laurila, T., Dada, L., Bezan-takos, S., Ahonen, L., Neitola, K., Maisser, A., Bimenyimana, E., Christodoulou, A., Unga, F., Savvides, C., Lehtipalo, K., Kangasluoma, J., Biskos, G., Petäjä, T., Kerminen, V.-M., Sciare, J., and Kulmala, M.: Towards understanding the characteristics of new particle formation in the Eastern Mediterranean, *Atmos. Chem. Phys.*, 21, 9223–9251, <https://doi.org/10.5194/acp-21-9223-2021>, 2021.
- Backman, J., Rizzo, L. V., Hakala, J., Nieminen, T., Manninen, H. E., Morais, F., Aalto, P. P., Siivola, E., Carbone, S., Hillamo, R., Artaxo, P., Virkkula, A., Petäjä, T., and Kulmala, M.: On the diurnal cycle of urban aerosols, black carbon and the occurrence of new particle formation events in spring-time São Paulo, Brazil, *Atmos. Chem. Phys.*, 12, 11733–11751, <https://doi.org/10.5194/acp-12-11733-2012>, 2012.
- Bianchi, F., Tröstl, J., Junninen, H., Frege, C., Henne, S., Hoyle, C. R., Molteni, U., Herrmann, E., Adamov, A., Bukowiecki, N., Chen, X., Duplissy, J., Gysel, M., Hutterli, M., Kangasluoma, J., Kontkanen, J., Kürten, A., Manninen, H. E., Münch, S., and Baltensperger, U.: New particle formation in the free troposphere: A question of chemistry and timing, *Science*, 352, 1109–1112, <https://doi.org/10.1126/science.aad5456>, 2016.
- Boulon, J., Sellegri, K., Hervo, M., and Laj, P.: Observations of nucleation of new particles in a volcanic plume, *P. Natl. Acad. Sci. USA*, 108, 12223–12226, <https://doi.org/10.1073/pnas.1104923108>, 2011.
- Bousiotis, D., Pope, F. D., Beddows, D. C. S., Dall'Osto, M., Massling, A., Nøjgaard, J. K., Nordstrøm, C., Niemi, J. V., Portin, H., Petäjä, T., Perez, N., Alastuey, A., Querol, X., Kouvarakis, G., Mihalopoulos, N., Vratolis, S., Eleftheriadis, K.,

- Wiedensohler, A., Weinhold, K., Merkel, M., Tuch, T., and Harrison, R. M.: A phenomenology of new particle formation (NPF) at 13 European sites, *Atmos. Chem. Phys.*, 21, 11905–11925, <https://doi.org/10.5194/acp-21-11905-2021>, 2021.
- Calidonna, C. R., Avolio, E., Gullì, D., Ammoscato, I., De Pino, M., Donato, A., and Lo Feudo, T.: Five Years of Dust Episodes at the Southern Italy GAW Regional Coastal Mediterranean Observatory: Multisensor and Modelling Analysis, *Atmosphere*, 11, 456, <https://doi.org/10.3390/atmos11050456>, 2020.
- Carslaw, D. C. and Ropkins, K.: openair – An R package for air quality data analysis, *Environ. Modell. Softw.*, 27/28, 52–61, <https://doi.org/10.1016/j.envsoft.2011.09.008>, 2012.
- Casquero-Vera, J. A., Lyamani, H., Dada, L., Hakala, S., Paa-sonen, P., Román, R., Fraile, R., Petäjä, T., Olmo-Reyes, F. J., and Alados-Arboledas, L.: New particle formation at urban and high-altitude remote sites in the south-eastern Iberian Peninsula, *Atmos. Chem. Phys.*, 20, 14253–14271, <https://doi.org/10.5194/acp-20-14253-2020>, 2020.
- Casquero-Vera, J. A., Lyamani, H., Titos, G., Minguillón, M. C., Dada, L., Alastuey, A., Querol, X., Petäjä, T., Olmo, F. J., and Alados-Arboledas, L.: Quantifying traffic, biomass burning and secondary source contributions to atmospheric particle number concentrations at urban and suburban sites, *Sci. Total Environ.*, 768, 145282, <https://doi.org/10.1016/j.scitotenv.2021.145282>, 2021.
- Conte, M., Merico, E., Cesari, D., Dinoi, A., Grasso, F. M., Donato, A., Guascito, M. R., and Contini, D.: Long-term characterisation of African dust advection in south-eastern Italy: Influence on fine and coarse particle concentrations, size distributions, and carbon content, *Atmos. Res.*, 233, 104690, <https://doi.org/10.1016/j.atmosres.2019.104690>, 2020.
- Cristofanelli, P., Busetto, M., Calzolari, F., Ammoscato, I., Gullì, D., Dinoi, A., Calidonna, C. R., Contini, D., Sferlazzo, D., Di Iorio, T., Piacentino, S., Marinoni, A., Maione, M., and Bonasoni, P.: Investigation of reactive gases and methane variability in the coastal boundary layer of the central Mediterranean basin, *Elem. Sci. Anthr.*, 5, 12, <https://doi.org/10.1525/elementa.216>, 2017.
- Cusack, M., Pérez, N., Pey, J., Alastuey, A., and Querol, X.: Source apportionment of fine PM and sub-micron particle number concentrations at a regional background site in the western Mediterranean: a 2.5 year study, *Atmos. Chem. Phys.*, 13, 5173–5187, <https://doi.org/10.5194/acp-13-5173-2013>, 2013.
- Dai, L., Wang, H. L., Zhou, L. Y., An, J. L., Tang, L. L., Lu, C. S., Yan, W. L., Liu, R. Y., Kong, S. F., Chen, M. D., Lee, S. H., and Yu, H.: Regional and local new particle formation events observed in the Yangtze River Delta region, China, *J. Geophys. Res.-Atmos.*, 122, 2389–2402, <https://doi.org/10.1002/2016JD026030>, 2017.
- Dal Maso, M., Kulmala, M., Riipinen, I., Wagner, R., Hussein, T., Aalto, P. P., and Lehtinen, K. E. J.: Formation and growth of fresh atmospheric aerosols: eight years of aerosol size distribution data from SMEAR II, Hyytiälä, Finland, *Boreal Environ. Res.*, 10, 323–336, 2005.
- Dall’Osto, M., Querol, X., Alastuey, A., O’Dowd, C., Harrison, R. M., Wenger, J., and Gómez-Moreno, F. J.: On the spatial distribution and evolution of ultrafine particles in Barcelona, *Atmos. Chem. Phys.*, 13, 741–759, <https://doi.org/10.5194/acp-13-741-2013>, 2013.
- Debevec, C., Sauvage, S., Gros, V., Sellegri, K., Sciare, J., Pikridas, M., Stavroulas, I., Leonardis, T., Gaudion, V., Depelchin, L., Fronval, I., Sarda-Esteve, R., Baisnée, D., Bonsang, B., Savvides, C., Vrekoussis, M., and Locoge, N.: Driving parameters of biogenic volatile organic compounds and consequences on new particle formation observed at an eastern Mediterranean background site, *Atmos. Chem. Phys.*, 18, 14297–14325, <https://doi.org/10.5194/acp-18-14297-2018>, 2018.
- De Reus, M., Dentener, F., Thomas, A., Borrmann, S., Strom, J., and Lelieveld, J.: Airborne observations of dust aerosol over the North Atlantic Ocean during ACE-2: indications for heterogeneous ozone destruction, *J. Geophys. Res.*, 105, 15263–15275, <https://doi.org/10.1029/2000JD900164>, 2000.
- Dinoi, A., Conte, M., Grasso, F. M., and Contini, D.: Long-term characterization of submicron atmospheric particles in an urban background site in Southern Italy, *Atmosphere*, 11, 334, <https://doi.org/10.3390/atmos11040334>, 2020.
- Dinoi, A., Weinhold, K., Wiedensohler, A., and Contini, D.: Study of new particle formation events in southern Italy, *Atmos. Environ.*, 244, 117920, <https://doi.org/10.1016/j.atmosenv.2020.117920>, 2021a.
- Dinoi, A., Gullì, D., Ammoscato, I., Calidonna, C. R., and Contini, D.: Impact of the coronavirus pandemic lockdown on atmospheric nanoparticle concentrations in two sites of Southern Italy, *Atmosphere*, 12, 352, <https://doi.org/10.3390/atmos12030352>, 2021b.
- Donato, A., Lo Feudo, T., Marinoni, A., Dinoi, A., Avolio, E., Merico, E., Calidonna, C. R., Contini, D., and Bonasoni, P.: Characterization of in situ aerosol optical properties at three observatories in the Central Mediterranean, *Atmosphere*, 9, 369, <https://doi.org/10.3390/atmos9100369>, 2018.
- Draxler, R. and Hess, G. D.: An overview of the HYSPLIT 4 modeling system for trajectories, dispersion and deposition, *Aust. Meteorol. Mag.*, 47, 295–308, 1998.
- Draxler, R. R. and Hess, G. D.: Description of the HYSPLIT 4 Modeling System, NOAA Technical Memorandum ERL ARL-224, <https://www.arl.noaa.gov/documents/reports/arl-224.pdf> (last access: 2020), 2004.
- Franco, M. A., Ditas, F., Krempner, L. A., Machado, L. A. T., Andreae, M. O., Araújo, A., Barbosa, H. M. J., de Brito, J. F., Carbone, S., Holanda, B. A., Morais, F. G., Nascimento, J. P., Pöhlker, M. L., Rizzo, L. V., Sá, M., Saturno, J., Walter, D., Wolff, S., Pöschl, U., Artaxo, P., and Pöhlker, C.: Occurrence and growth of sub-50 nm aerosol particles in the Amazonian boundary layer, *Atmos. Chem. Phys.*, 22, 3469–3492, <https://doi.org/10.5194/acp-22-3469-2022>, 2022.
- Fuchs, N. A. and Sutugin, A. G.: Highly dispersed aerosols, in: *Topics in Current Aerosol Research*, edited by: Hidy, G. M. and Brock, J. R., Pergamon, New York, p. 1, <https://doi.org/10.1016/B978-0-08-016674-2.50006-6>, 1971.
- Hussein, T., Molgaard, B., Hannuniemi, H., Martikainen, J., Järvi, L., Wegner, T., Ripamonti, G., Weber, S., Vesala, T., and Hämeri, K.: Fingerprints of the urban particle number size distribution in Helsinki, Finland: Local vs. regional characteristics, *Boreal Environ. Res.*, 19, 1–20, 2014.
- Hussein, T., Atashi, N., Sogacheva, L., Hakala, S., Dada, L., Petäjä, T., and Kulmala, M.: Characterization of Urban New Particle Formation in Amman–Jordan, *Atmosphere*, 11, 79, <https://doi.org/10.3390/atmos11010079>, 2020.

- Jensen, D. D., Price, T. A., Nadeau, D. F., Kingston, J., and Pardyjak, E. R.: Coastal Wind and Turbulence Observations during the Morning and Evening Transitions over Tropical Terrain, *J. Appl. Meteorol. Clim.*, 56, 3167–3185, <https://doi.org/10.1175/JAMC-D-17-0077.1>, 2017.
- Jokinen, T., Lehtipalo, K., Thakur, R. C., Ylivinkka, I., Neitola, K., Sarnela, N., Laitinen, T., Kulmala, M., Petäjä, T., and Sipilä, M.: Measurement report: Long-term measurements of aerosol precursor concentrations in the Finnish subarctic boreal forest, *Atmos. Chem. Phys.*, 22, 2237–2254, <https://doi.org/10.5194/acp-22-2237-2022>, 2022.
- Kalivitis, N., Kerminen, V.-M., Kouvarakis, G., Stavroulas, I., Tzitzikalaki, E., Kalkavouras, P., Daskalakis, N., Myriokefalitakis, S., Bougiatioti, A., Manninen, H. E., Roldin, P., Petäjä, T., Boy, M., Kulmala, M., Kanakidou, M., and Mihalopoulos, N.: Formation and growth of atmospheric nanoparticles in the eastern Mediterranean: results from long-term measurements and process simulations, *Atmos. Chem. Phys.*, 19, 2671–2686, <https://doi.org/10.5194/acp-19-2671-2019>, 2019.
- Kalkavouras, P., Bougiatioti, A., Grivas, G., Stavroulas, I., Kalivitis, N., Liakakou, E., Gerasopoulos, E., Pilinis, C., and Mihalopoulos, N.: On the regional aspects of new particle formation in the Eastern Mediterranean: A comparative study between a background and an urban site based on long term observations, *Atmos. Res.*, 239, 104911, <https://doi.org/10.1016/j.atmosres.2020.104911>, 2020.
- Kerminen, V.-M., Chen, X., Vakkari, V., Petäjä, T., Kulmala, M., and Bianchi, F.: Atmospheric new particle formation and growth: Review of field observations, *Environ. Res. Lett.*, 13, 103003, <https://doi.org/10.1088/1748-9326/aadf3c>, 2018.
- Kopanakis, I., Chatoutsidou, S. E., Torseth, K., Glytsos, T., and Lazaridis, M.: Particle number size distribution in the eastern Mediterranean: Formation and growth rates of ultrafine airborne atmospheric particles, *Atmos. Environ.*, 77, 790–802, <https://doi.org/10.1016/j.atmosenv.2013.05.066>, 2013.
- Kulmala, M., Petäjä, T., Nieminen, T., Sipilä, M., Manninen, H. E., Lehtipalo, K., Dal Maso, M., Aalto, P. P., Junninen, H., Paasonen, P., Riipinen, I., Lehtinen, K. E. J., Laaksonen, A., and Kerminen, V.-M.: Measurement of the nucleation of atmospheric aerosol particles, *Nat. Protoc.*, 7, 1651–1667, <https://doi.org/10.1038/nprot.2012.091>, 2012.
- Lehtinen, K. E. J. and Kulmala, M.: A model for particle formation and growth in the atmosphere with molecular resolution in size, *Atmos. Chem. Phys.*, 3, 251–257, <https://doi.org/10.5194/acp-3-251-2003>, 2003.
- Merikanto, J., Spracklen, D. V., Mann, G. W., Pickering, S. J., and Carslaw, K. S.: Impact of nucleation on global CCN, *Atmos. Chem. Phys.*, 9, 8601–8616, <https://doi.org/10.5194/acp-9-8601-2009>, 2009.
- Minguillón, M. C., Ripoll, A., Pérez, N., Prévôt, A. S. H., Canonaco, F., Querol, X., and Alastuey, A.: Chemical characterization of submicron regional background aerosols in the western Mediterranean using an Aerosol Chemical Speciation Monitor, *Atmos. Chem. Phys.*, 15, 6379–6391, <https://doi.org/10.5194/acp-15-6379-2015>, 2015.
- Mirme, S., Mirme, A., Minikin, A., Petzold, A., Hörrak, U., Kerminen, V.-M., and Kulmala, M.: Atmospheric sub-3 nm particles at high altitudes, *Atmos. Chem. Phys.*, 10, 437–451, <https://doi.org/10.5194/acp-10-437-2010>, 2010.
- Ndour, M., Conchon, P., D’Anna, B., Ka, O., and George, C.: Photochemistry of mineral dust surface as a potential atmospheric renoxification process, *Geophys. Res. Lett.*, 36, 5, <https://doi.org/10.1029/2008GL036662>, 2009.
- Németh, Z. and Salma, I.: Spatial extension of nucleating air masses in the Carpathian Basin, *Atmos. Chem. Phys.*, 14, 8841–8848, <https://doi.org/10.5194/acp-14-8841-2014>, 2014.
- Nemeth, Z., Rosat, B., Zikova, N., Salma, I., Bozo, L., de Espana, C. D., Schwarz, J., Zdimal, V., and Wonaschütz, A.: Comparison of atmospheric new particle formation events in three Central European cities, *Atmos. Environ.*, 178, 191–197, <https://doi.org/10.1016/j.atmosenv.2018.01.035>, 2018.
- Nieminen, T., Kerminen, V.-M., Petäjä, T., Aalto, P. P., Arshinov, M., Asmi, E., Baltensperger, U., Beddows, D. C. S., Beukes, J. P., Collins, D., Ding, A., Harrison, R. M., Henzing, B., Hooda, R., Hu, M., Hörrak, U., Kivekäs, N., Komsaare, K., Krejci, R., Kristensson, A., Laakso, L., Laaksonen, A., Leaitch, W. R., Lihavainen, H., Mihalopoulos, N., Németh, Z., Nie, W., O’Dowd, C., Salma, I., Sellegri, K., Svenningsson, B., Swietlicki, E., Tunved, P., Ulevicius, V., Vakkari, V., Vana, M., Wiedensohler, A., Wu, Z., Virtanen, A., and Kulmala, M.: Global analysis of continental boundary layer new particle formation based on long-term measurements, *Atmos. Chem. Phys.*, 18, 14737–14756, <https://doi.org/10.5194/acp-18-14737-2018>, 2018.
- Petäjä, T., Mauldin, III, R. L., Kosciuch, E., McGrath, J., Nieminen, T., Paasonen, P., Boy, M., Adamov, A., Kotiaho, T., and Kulmala, M.: Sulfuric acid and OH concentrations in a boreal forest site, *Atmos. Chem. Phys.*, 9, 7435–7448, <https://doi.org/10.5194/acp-9-7435-2009>, 2009.
- Pikridas, M., Vrekoussis, M., Sciare, J., Kleanthous, S., Vasiladou, E., Kizas, C., Savvides, C., and Mihalopoulos, N.: Spatial and temporal (short and long-term) variability of submicron, fine and sub-10 μm particulate matter (PM₁, PM_{2.5}, PM₁₀) in Cyprus, *Atmos. Environ.*, 191, 79–93, <https://doi.org/10.1016/j.atmosenv.2018.07.048>, 2018.
- Putaud, J.-P., Van Dingenen, R., Alastuey, A., Bauer, H., Birmili, W., Cyrys, J., Flentje, H., Fuzzi, S., Gehrig, R., Hansson, H.C., Harrison, R.M., Herrmann, H., Hitznerberger, R., Hüglin, C., Jones, A.M., Kasper-Giebl, A., Kiss, G., Kousa, A., Kuhlbusch, T.A.J., Löschau, G., Maenhaut, W., Molnar, A., Moreno, T., Pekkanen, J., Perrino, C., Pitz, M., Puxbaum, H., Querol, X., Rodriguez, S., Salma, I., Schwarz, J., Smolik, J., Schneider, J., Spindler, G., ten Brink, H., Tursic, J., Viana, M., Wiedensohler, A., and Raes, F.: A European aerosol phenomenology – 3: Physical and chemical characteristics of particulate matter from 60 rural, urban, and kerbside sites across Europe, *Atmos. Environ.*, 44, 1308–1320, <https://doi.org/10.1016/j.atmosenv.2009.12.011>, 2010.
- Querol, X., Gangoiti, G., Mantilla, E., Alastuey, A., Minguillón, M. C., Amato, F., Reche, C., Viana, M., Moreno, T., Karanasiou, A., Rivas, I., Pérez, N., Ripoll, A., Brines, M., Ealo, M., Pandolfi, M., Lee, H.-K., Eun, H.-R., Park, Y.-H., Escudero, M., Beddows, D., Harrison, R. M., Bertrand, A., Marchand, N., Lyasota, A., Codina, B., Olid, M., Udina, M., Jiménez-Esteve, B., Soler, M. R., Alonso, L., Millán, M., and Ahn, K.-H.: Phenomenology of high-ozone episodes in NE Spain, *Atmos. Chem. Phys.*, 17, 2817–2838, <https://doi.org/10.5194/acp-17-2817-2017>, 2017.

- Rose, C., Sellegri, K., Velarde, F., Moreno, I., Ramonet, M., Weinhold, K., Krejci, R., Ginot, P., Andrade, M., Wiedensohler, A., and Laj, P.: Frequent nucleation events at the high altitude station of Chacaltaya (5240 m a.s.l.), Bolivia, *Atmos. Environ.*, 102, 18–29, <https://doi.org/10.1016/j.atmosenv.2014.11.015>, 2015.
- Saha, P. K., Robinson, E. S., Shah, R. U., Zimmerman, N., Apte, J. S., Robinson, A. L., and Presto, A. A.: Reduced ultrafine particle concentration in urban air: changes in nucleation and anthropogenic emissions, *Environ. Sci. Technol.*, 52, 6798–6806, <https://doi.org/10.1021/acs.est.8b00910>, 2018.
- Salma, I. and Németh, Z.: Dynamic and timing properties of new aerosol particle formation and consecutive growth events, *Atmos. Chem. Phys.*, 19, 5835–5852, <https://doi.org/10.5194/acp-19-5835-2019>, 2019.
- Salma, I., Németh, Z., Kerminen, V.-M., Aalto, P., Nieminen, T., Weidinger, T., Molnár, Á., Imre, K., and Kulmala, M.: Regional effect on urban atmospheric nucleation, *Atmos. Chem. Phys.*, 16, 8715–8728, <https://doi.org/10.5194/acp-16-8715-2016>, 2016.
- Salma, I., Varga, V., and Németh, Z.: Quantification of an atmospheric nucleation and growth process as a single source of aerosol particles in a city, *Atmos. Chem. Phys.*, 17, 15007–15017, <https://doi.org/10.5194/acp-17-15007-2017>, 2017.
- Sartelet, K., Kim, Y., Couvidat, F., Merkel, M., Petäjä, T., Sciare, J., and Wiedensohler, A.: Influence of emission size distribution and nucleation on number concentrations over Greater Paris, *Atmos. Chem. Phys.*, 22, 8579–8596, <https://doi.org/10.5194/acp-22-8579-2022>, 2022.
- Schroder, F. and Strom, J.: Aircraft measurements of sub-micrometer aerosol particles (> 7 m) in the mid-latitude free troposphere and troposphere region, *Atmos. Res.*, 44, 333–356, [https://doi.org/10.1016/S0169-8095\(96\)00034-8](https://doi.org/10.1016/S0169-8095(96)00034-8), 1997.
- Sipilä, M., Berndt, T., Petäjä, T., Brus, D., Vanhanen, J., Stratmann, F., Patokoski, J., Mauldin, R. L., Hyvärinen, A.-P., Lihavainen, H., and Kulmala, M.: The Role of Sulfuric Acid in Atmospheric Nucleation, *Science*, 327, 1243–1246, <https://doi.org/10.1126/science.1180315>, 2010.
- Stohl, A., Hittenberger, M., and Wotawa, G.: Validation of the Lagrangian particle dispersion model FLEXPART against large scale tracer experiment data, *Atmos. Environ.*, 32, 4245–4264, [https://doi.org/10.1016/S1352-2310\(98\)00184-8](https://doi.org/10.1016/S1352-2310(98)00184-8), 1998.
- Wehner, B., Werner, F., Ditas, F., Shaw, R. A., Kulmala, M., and Siebert, H.: Observations of new particle formation in enhanced UV irradiance zones near cumulus clouds, *Atmos. Chem. Phys.*, 15, 11701–11711, <https://doi.org/10.5194/acp-15-11701-2015>, 2015.
- Wiedensohler, A., Birmili, W., Nowak, A., Sonntag, A., Weinhold, K., Merkel, M., Wehner, B., Tuch, T., Pfeifer, S., Fiebig, M., Fjåraa, A. M., Asmi, E., Sellegri, K., Depuy, R., Venzac, H., Villani, P., Laj, P., Aalto, P., Ogren, J. A., Swietlicki, E., Williams, P., Roldin, P., Quincey, P., Hüglin, C., Fierz-Schmidhauser, R., Gysel, M., Weingartner, E., Riccobono, F., Santos, S., Grünig, C., Faloon, K., Beddows, D., Harrison, R., Monahan, C., Jennings, S. G., O'Dowd, C. D., Marinoni, A., Horn, H.-G., Keck, L., Jiang, J., Scheckman, J., McMurry, P. H., Deng, Z., Zhao, C. S., Moerman, M., Henzing, B., de Leeuw, G., Löschau, G., and Bastian, S.: Mobility particle size spectrometers: harmonization of technical standards and data structure to facilitate high quality long-term observations of atmospheric particle number size distributions, *Atmos. Meas. Tech.*, 5, 657–685, <https://doi.org/10.5194/amt-5-657-2012>, 2012.
- Wonaschütz, A., Demattio, A., Wagner, R., Burkart, J., Zíková, N., Vodička, P., Ludwig, W., Steiner, G., Schwarz, J., and Hitznerberger, R.: Seasonality of new particle formation in Vienna, Austria – influence of air mass origin and aerosol chemical composition, *Atmos. Environ.*, 118, 118–126, <https://doi.org/10.1016/j.atmosenv.2015.07.035>, 2015.
- Wu, H., Li, Z., Li, H., Luo, K., Wang, Y., Yan, P., Hu, F., Zhang, F., Sun, Y., Shang, D., Liang, C., Zhang, D., Wei, J., Wu, T., Jin, X., Fan, X., Cribb, M., Fischer, M. L., Kulmala, M., and Petäjä, T.: The impact of the atmospheric turbulence-development tendency on new particle formation: a common finding on three continents, *Nat. Sci. Rev.*, 8, nwaa157, <https://doi.org/10.1093/nsr/nwaa157>, 2021.
- Yadav, S. K., Kompalli, S. K., Gurjar, B. R., and Mishra, R. K.: Aerosol number concentrations and new particle formation events over a polluted megacity during the COVID-19 lockdown, *Atmos. Environ.*, 259, 118526, <https://doi.org/10.1016/j.atmosenv.2021.118526>, 2021.
- Yu, F., Luo, G., Nair, A. A., Schwab, J. J., Sherman, J. P., and Zhang, Y.: Wintertime new particle formation and its contribution to cloud condensation nuclei in the Northeastern United States, *Atmos. Chem. Phys.*, 20, 2591–2601, <https://doi.org/10.5194/acp-20-2591-2020>, 2020.
- Zhang, Q. J., Beekmann, M., Freney, E., Sellegri, K., Pichon, J. M., Schwarzenboeck, A., Colomb, A., Bourriane, T., Michoud, V., and Borbon, A.: Formation of secondary organic aerosol in the Paris pollution plume and its impact on surrounding regions, *Atmos. Chem. Phys.*, 15, 13973–13992, <https://doi.org/10.5194/acp-15-13973-2015>, 2015.
- Zhu, Y. J., Sabaliauskas, K., Liu, X.H., Meng, H., Gao, H. W., Jeong, C.-H., Evans, G., and Yao, X. H.: Comparative analysis of new particle formation events in less and severely polluted urban atmosphere, *Atmos. Environ.*, 98, 655–664, <https://doi.org/10.1016/j.atmosenv.2014.09.043>, 2014.